Dynamics of Stiff-Chain Polymers in Isotropic Solution. 3. Flexibility Effect

Takahiro Sato,* Yasushi Takada, and Akio Teramoto

Department of Macromolecular Science, Osaka University, Toyonaka, Osaka 560, Japan

Received January 31, 1991; Revised Manuscript Received June 25, 1991

ABSTRACT: The rotational and longitudinal diffusion coefficients (D_r and $D_\parallel$) of stiff-chain polymers in isotropic solution dilute through concentrated are formulated on the basis of the rod theories by replacing the stiff chain by the "fuzzy cylinder" model. The equation for D_r is derived by a mean-field Green function method, while that for $D_\parallel$ is derived by two different methods: a Green function method and a hole theory. The expressions of D_r and $D_\parallel$ derived give two equations of the zero-shear viscosity (η_0) for stiff polymer solutions. The viscosity equation given by the $D_\parallel$ from the hole theory describes well the dependence of η_0 on polymer concentration c and molecular weight M for isotropic solutions of two rigid polysaccharides over the entire ranges of c and M examined, when the "critical hole", which is necessary for the longitudinal diffusion of the polymer, has a shape similar to the fuzzy cylinder, whereas the other is applicable only for low molecular weight samples whose conformations are close to rigid rods.

1. Introduction

As demonstrated experimentally in the preceding paper[1] (Part 2 of this series), as well as the work of Enomoto et al.,[2] the zero-shear viscosity η_0 of stiff-chain polymer solutions is remarkably affected by the chain flexibility. Similar flexibility effects are also reported on the rotational diffusion coefficient of stiff chains in semidilute solution by Maguire et al.[3] and Zero and Pecora.[4]

On the other hand, theoretically, the flexibility effect on the stiff-chain polymer dynamics in concentrated isotropic solution has been treated by Odijk[5] and Doi.[6] In 1983, Odijk made a scaling argument on the dynamics (the rotational relaxation) of entangled wormlike chains, using a virtual tube model and introducing the "deflection length". However, he dealt only with the case of very concentrated solutions or tight networks where the diameter of the virtual tube is much smaller than the persistence length q of the wormlike chain. Afterward, Doi presented a more rigorous calculation of the rotational diffusion coefficient D_r as well as the translational diffusion coefficient D_t of wormlike chains in network or concentrated solution. However, in this theory, he assumed the chain to move only along its contour (i.e., neglected the lateral fluctuation of the chain conformation in the virtual tube), which restricted his theory also to very concentrated solutions or tight networks.

It is well-known that a stiff-chain polymer solution is transformed into a liquid crystal above a critical concentration, which is remarkably low for sufficiently stiff polymers.[7] Therefore, Odijk's and Doi's assumption is not necessarily acceptable for isotropic solutions of stiff polymers. Indeed their theories predict that D_r of semiflexible polymers is independent of the polymer concentration, which obviously disagrees with experimental results for stiff polymers in semidilute solution.[3,4,8,9]

In contrast with Doi's model, we here assume that the internal motion of the stiff chain can occur rapidly and freely even in entangled polymer solutions. This assumption may be accepted for stiffer polymer chains in less concentrated solutions. In this situation and after the chain motion is averaged over a certain time scale, the segments of one stiff chain are distributed in a cylindrical symmetry (see Figure 1). Thus, the global motion of the stiff chain may be identified with that of a segment-distribution model with a cylindrical symmetry, called the "fuzzy cylinder" model and specified in more detail in section 2. With this model, we consider the entanglement effect on D_r, as well as the jamming effect on the longitudinal diffusion coefficient $D_\parallel$, for the stiff chain in isotropic solution in sections 3 and 4. The formulation procedure of D_r is similar to that used in the previous paper[10] (Part 1 of this series) for the rodlike polymer. We treat $D_\parallel$ of stiff chains by two methods, a mean-field Green function method and a hole theory. The former was originally used by Edwards and Evans[11] to formulate $D_\parallel$ of the rodlike polymer, while the latter was used by Cohen and Turnbull[12] to analyze the self-diffusion in small molecular fluids.

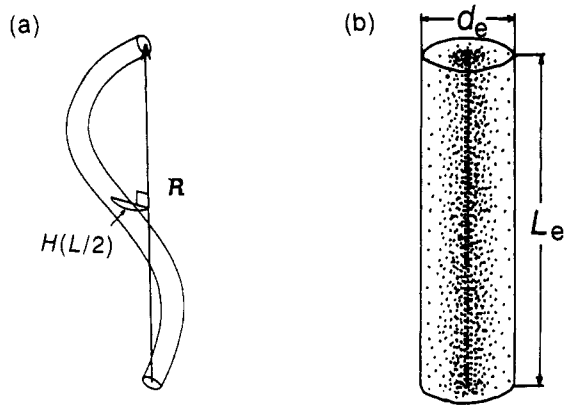

Figure 1. Two models for the semiflexible polymer: (a) the wormlike cylinder model and (b) the fuzzy cylinder model.

If the contribution of the chain internal motion to the solution viscosity is neglected, the equation of η_0 for the polymer solution is given from expressions of D_r and $D_\parallel$, as described in section 5; we obtain two viscosity equations from two different expressions of $D_\parallel$. Section 6 tests these equations with the experimental results for η_0 of isotropic solutions of two rigid helical polysaccharides, xanthan[1] and schizophyllan.[2]

In the formulations of the above dynamic quantities, we need several transport coefficients at infinite dilution. We use for them the corresponding quantities of wormlike cylinders (not of fuzzy cylinders) with some approximations. The finite thickness effect of the chain on the transport coefficients, which has been neglected in Part 1, is taken into account in this study, while the hydrodynamic screening effect at finite concentration is neglected as before. Recently Altenberger et al.[13] has

0024-9297/91/2224-6220$02.50/0

concluded theoretically that the hydrodynamic screening vanishes for stationary flows (or quiescent states). Their conclusion, which justifies our neglect of the screening, is still in dispute with diametrically opposed conclusions of other investigators.[14-17]

2. Model

As schematically shown in Figure 1, the wormlike cylinder with the contour length L and diameter d is identified with a fuzzy cylinder model to formulate global dynamic properties of the stiff chain. The cylindrical axis of the model is defined as the direction of the end-to-end vector **R**. Thus the length L_e of the fuzzy cylinder model is equated to the root-mean-square end-to-end distance $\langle R^2\rangle^{1/2}$. We use the equation of $\langle R^2\rangle^{1/2}$ for the wormlike (or the Kratky–Porod) chain.[18] The effective diameter d_e of the fuzzy cylinder model may be estimated by

$$d_e = [\langle H(L/2)^2\rangle + d^2]^{1/2} \tag{1}$$

where $\langle H(L/2)^2\rangle$ is the mean-square distance of the chain midpoint from the end-to-end displacement axis, as illustrated in Figure 1a. Since $\langle H(L/2)^2\rangle$ for the wormlike chain model has not been obtained, we use Hoshikawa et al.'s results[19] for $\langle H(L/2)^2\rangle$ calculated by using Tagami's model[20] for the stiff chain. Although Tagami's model permits the stretch of the chain contour in contrast with the wormlike chain, both models give identical expressions of $\langle R^2\rangle$ and the mean-square radius of gyration, so that Hoshikawa et al.'s $\langle H(L/2)^2\rangle$ is expected to be a good approximation to that of the wormlike chain. In the coil limit, $\langle H(L/2)^2\rangle$ becomes equal to $\langle R^2\rangle/6$.

To consider the entanglement and jamming effects, we need information about the interaction between two fuzzy cylinders. To a first approximation, we assume a hard-core interaction between fuzzy cylinders, which acts as an infinite repulsive interaction when the shortest distance between two cylinders is shorter than d_c but exhibits no interaction otherwise. The value of d_c should take some value between 0 and d_e.

Many years ago, Hearst[21] used a segment-distribution model with a cylindrical symmetry to formulate transport coefficients of a stiff chain *at infinite dilution*. Thus, he is the pioneer of the application of the cylindrical segment-distribution model to the stiff-chain dynamics. However, he chose the direction of the tangent to the chain at the midpoint of its contour as the cylindrical axis of the model, so that his model differs from ours.

3. Rotational Diffusion Coefficient

At a finite concentration, the rotational motion of stiff chains is hindered by collision with surrounding chains. This entanglement effect slows down the rotational diffusion of the chain. Recently Teraoka and Hayakawa[22] have considered this entanglement effect to formulate the rotational diffusion coefficient D_r for the rodlike polymer in dilute through semidilute solutions by use of a mean-field Green function formulation; in Part 1[10] of this series, their formulation has been extended to more concentrated solutions, where the jamming effect on the longitudinal diffusion of the rod becomes important. It is not difficult to apply this method to isotropic solutions of fuzzy cylinders from dilute to concentrated, as shown below.

We follow Teraoka and Hayakawa to consider a sphere S_t of radius L_e centered on the center of mass of a test cylinder (the cylinder in consideration) and project the test cylinder and all portions of the surrounding cylinders

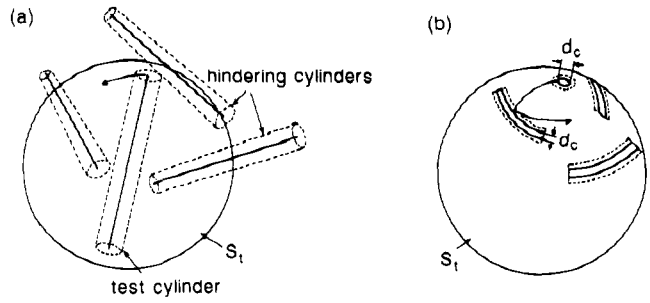

Figure 2. (a) Rotational diffusion process of the test cylinder hindered by surrounding cylinders intersecting with the sphere S_t. (b) Projection of the test and hindering cylinders onto the sphere S_t.

intersecting with the sphere S_t onto the spherical surface. The projections of the test cylinder and surrounding cylinders are a circle and ribbons, respectively (see Figure 2), and rotational diffusion of the test cylinder can be identified with the two-dimensional (translational) diffusion of the circle interacting with ribbonlike obstacles on the spherical surface.

The circle and ribbons on the spherical surface possess hard cores of the thickness d_c because of the definition of the fuzzy cylinder. Further, the ribbons are regarded as reflecting barriers. Then we can evaluate the mean-field Green function subjected to multiple perturbation, following the previous work.[22] (Here the reflection of the circle at two ends of the ribbon is neglected.) The perturbed Green function yields D_r for the fuzzy cylinder model as

$$\frac{D_r}{D_{r0}} = \left[1 + \frac{2}{3\sqrt{\pi}}\bar{f}_c\langle b\rangle\tau^{3/2}D_{r0}^{1/2}\right]^{-2} \tag{2}$$

where $\bar{f}_c$ is the number of barriers per unit solid angle appearing on the surface of sphere S_t per unit time interval, $\langle b\rangle$ is the average central angle subtended by the ribbon, and τ is the mean lifetime of the barrier; the subscript 0 indicates the quantity at infinite dilution. The quantity $\bar{f}_c$ is proportional to N_b/τ, where N_b is the average number of surrounding cylinders whose hard cores are intersecting with the sphere S_t at a given instance. From the mutual excluded volume between the sphere S_t and a surrounding cylinder core,[23] we may obtain

$$N_b = \frac{5\pi}{12}L_e^3 f(L_e/d_c)c' \tag{3}$$

where c' is the number density of the chain in the solution and $f(x)$ is

$$f(x) = (1 + 1/x)^2(1 - 1/5x) \tag{4}$$

(In this derivation, the surrounding cylinder core is assumed to be a spherocylinder with the length L_e and the diameter d_c.) The function $f(L_e/d_c)$ varies between 1 and 1.821 because $L_e/d_c \geq L_e/d_e \geq \sqrt{6}$.

The appearance and disappearance of barriers on the surface of the sphere S_t are caused predominantly by the longitudinal diffusion of the hindering cylinders and/or the test cylinder. Therefore, τ may be equated to the average time, which the cylinders take to diffuse longitudinally a distance on the order of L_e, and given by

$$\tau \propto L_e^2/D_\parallel \tag{5}$$

Using eqs 3 and 5, we may rewrite eq 2 as

$$D_r/D_{r0} = [1 + Bc'(D_{\parallel 0}/D_\parallel)^{1/2}]^{-2} \tag{6}$$

where

$$B = \beta^{-1/2} L_e^3 f(L_e/d_c)(L_e^2 D_{r0}/6D_{\parallel 0})^{1/2} \quad (7)$$

with a numerical constant β, which is independent of c' and L. Teraoka et al.[24] estimated β to be 1350 for the infinitely thin rod from a detailed geometrical consideration on the calculation with a tube model.

To complete the formulation of D_r, the expressions for the two ratios $D_{r0}/D_{\parallel 0}$ and $D_{\parallel 0}/D_{\parallel}$ are needed. The former is an infinite-dilution quantity and is calculated by using the wormlike cylinder model (see eqs A6 and A11 in Appendix A), while the latter is formulated in the next section.

4. Longitudinal Diffusion Coefficient

The longitudinal diffusion, as well as the rotational diffusion, of the stiff-chain polymer must be perturbed by surrounding polymers in a moderately concentrated solution (the jamming effect). Therefore, $D_{\parallel}$ should decrease from $D_{\parallel 0}$ with increasing polymer concentration. In Part 1,[10] we have obtained an expression of $D_{\parallel}$ for rodlike polymers by modifying the Green function method of Edwards and Evans,[11] where the hindrance of the longitudinal motion of a test rod was assumed to be released only by the longitudinal diffusion of the hindering rods. If this assumption is valid to the fuzzy cylinder system, we can apply the same method to it and obtain

$$D_{\parallel}/D_{\parallel 0} = (1 - \alpha^{-1} L_e^2 d_c c')^2 \quad (8a)$$

where α is a numerical constant.

We can also formulate $D_{\parallel}$ for stiff chains by another method, the hole theory. This method is similar to that used by Cohen and Turnbull[12] to obtain an expression of the self-diffusion coefficient in liquids of small molecules and metals. The basic assumption in our hole theory is that the longitudinal diffusion of a test chain occurs only when a "hole" that is larger than a critical hole exists in front of the test chain. Here the hole means a region that contains no chain segments in the solution (not true vacuum region), and then one should not confuse that with the free volume that often appears in the literature on polymer melts and solutions.

From Cohen and Turnbull's argument, it turns out that $D_{\parallel}$ is proportional to the total probability P_h of finding a hole that is larger than the critical hole. Thus the problem is to obtain this probability. Many years ago, Ogston[25] calculated the probability that corresponds to P_h for the case that the critical hole is spherical and the solute is rodlike. His calculation can be easily extended to the case of any shapes of the hole and solute;[26] P_h is written in terms of the average mutual excluded volume V_{ex}^* between the critical hole and the solute molecule as[27]

$$P_h = \exp(-V_{ex}^* c') \quad (9)$$

From this equation, $D_{\parallel}$ is written as

$$D_{\parallel} = D_{\parallel 0} \exp(-V_{ex}^* c') \quad (8b)$$

The explicit form of V_{ex}^* is given only when the shape and size of the critical hole is specified, which will be discussed in section 6.

For rodlike polymer solutions, the liquid crystal phase appears at $c' = 4.25/(L^2 d)$,[23] while α has been estimated in Part 1 to be ca. 13.[10] Therefore, the second term in the parentheses of eq 8a does not exceed 0.33, as far as we are concerned with the isotropic rodlike polymer solutions. The difference between $(1-x)^2$ and $\exp(-2x)$ is quite small, within $0 < x < 0.33$, and then eqs 8a and 8b give almost identical concentration dependences of $D_{\parallel}$ for these solutions. On the other hand, the difference between eqs 8a and 8b in the concentration dependence may become appreciable with increasing chain flexibility, because the flexibility makes the phase boundary concentration deviate upward from the Onsager prediction,[28] and the concentration range (or the range of x) of the isotropic phase region may be wide enough to distinguish between the functions $(1-x)^2$ and $\exp(-2x)$.

5. Zero-Shear Viscosity

As shown in Appendix B, the zero-shear viscosity η_0 of an isotropic solution of rodlike (spherocylindrical) polymers with finite thickness is related to D_r of the rod by

$$\eta_0 = \eta_s + (4\gamma^{-1} - 3\chi^2)\frac{c' k_B T}{30 D_{r0}} + \chi^2 \frac{c' k_B T}{10 D_r} \quad (10)$$

where η_s is the solvent viscosity, k_B the Boltzmann constant, and T the absolute temperature; the correction factors γ and χ for the finite thickness of the rod defined in the paper of Yoshizaki and Yamakawa[29] are known functions of the polymer axial ratio p (see eqs A10 and B2 in Appendixes A and B). With increasing p, the factors γ and χ approach unity, and eq 10 is reduced to eq B1 obtained by Doi and Edwards.[17] The first and second terms on the right-hand side of eq 10 come from the hydrodynamic energy dissipation due to the friction in solvent and between the polymer and solvent, respectively, while the third term originates from the orientational entropy loss of rods by the shear flow and represents the contribution of the end-over-end rotation of the rod to the viscosity. The second term has been derived by neglecting the hydrodynamic screening effect.

Our next task is to derive the corresponding relation for the isotropic solution of the semiflexible polymer. If the polymer has internal degrees of freedom, the internal motion of the polymer may contribute to η_0. Indeed, Nagasaka and Yamakawa[30] showed that the intrinsic viscosity $[\eta]$ of the elastic trumbbell near the rod limit consists of three terms; the two terms correspond to the second and third terms of eq 10, and the remaining term represents the contribution of the trumbbell bending motion to the viscosity. It is, however, very difficult to treat the dynamics of the internal motion of stiff chains, not only in concentrated solution but also even in dilute solution.

In the present derivation, we neglect the contribution of the chain internal motion and apply eq 10 as it is to the isotropic solution of stiff chains. This procedure may be justified for the following reason. Viscosity terms corresponding to the chain internal motions should be proportional to the relaxation times of the internal motion modes,[30,31] which are much shorter than the end-over-end rotational relaxation time ($\sim 1/D_r$), making these terms much smaller than the third term of eq 10. The difference between the end-over-end rotational and the internal relaxation times must be larger for stiffer chains in more concentrated solutions, so that eq 10 becomes more relevant to stiff polymer solutions in such a case.

Using eq A10, we rewrite eq 10 in the form

$$\eta_c \equiv \frac{(\eta_0 - \eta_s)/\eta_s}{c[\eta]} = 1 - \frac{3}{4}\gamma\chi^2 + \frac{3}{4}\gamma\chi^2 \frac{D_{r0}}{D_r} \quad (11)$$

where c is the polymer mass concentration ($=c'M/N_A$; M, the molecular weight of the polymer; N_A, Avogadro's

number). Combining eq 11 with eq 6, we finally obtain the following viscosity equation for semiflexible polymer solutions:

$$\eta_c = 1 - \frac{3}{4}\gamma\chi^2 + \frac{3}{4}\gamma\chi^2\left[1 + Bc'\left(\frac{D_{\parallel 0}}{D_\parallel}\right)^{1/2}\right]^2 \quad (12)$$

Either eq 8a or eq 8b may be used for $D_{\parallel 0}/D_\parallel$. In the rod limit, eq 12 becomes identical with the viscosity equation derived in Part 1,[10] if eq 8a is inserted into it and the finite thickness effects of rods are neglected (i.e., $\gamma = \chi = 1$, and eqs A1 and A2 are used instead of eqs A6 and A11).

When polymers with different stiffnesses are analyzed in terms of the wormlike chain model, it is convenient to measure all the lengths concerned with polymer chains in units of the Kuhn statistical segment length $2q$ where q is the persistence length. To avoid confusion, reduced quantities are denoted by symbols with tildes; for example, $\tilde{L}_e = L_e/(2q)$, $\tilde{B} = B/(2q)^3$, $\tilde{V}_{ex}^* = V_{ex}^*/(2q)^3$, $\tilde{c}' = (2q)^3c'$, and so on; only the reduced contour length identical with the number of the Kuhn segments is denoted by N ($\equiv\tilde{L}$). Using these reduced quantities along with the new reduced viscosity H_e defined by

$$H_e = \frac{4(\eta_c - 1)}{3\gamma\chi^2} + 1 \quad (13)$$

eq 12 with eq 8a can be rewritten as

$$\frac{\tilde{c}'}{H_e^{1/2} - 1} = \frac{1}{\tilde{B}}(1 - \alpha^{-1}\tilde{L}_e^{\,2}\tilde{d}_c\tilde{c}') \quad (14a)$$

and that with eq 8b as

$$\ln\left(\frac{H_e^{1/2} - 1}{\tilde{c}'}\right) = \ln\tilde{B} + \frac{1}{2}\tilde{V}_{ex}^*\tilde{c}' \quad (14b)$$

The quantity $\tilde{B}$ can be evaluated by eq 7 combined with eqs A6 and A11, resulting in

$$\tilde{B} = \beta^{-1/2}\tilde{L}_e^{\,3}f(L_e/d_c)\frac{\tilde{L}_e}{N}\left[\frac{F_r(p,N)}{F_\parallel(p,N)}\right]^{-1/2} \quad (15)$$

where $F_r(p,N)$ and $F_\parallel(p,N)$ are given by eqs A7 and A12, respectively ($p = L/d = N/\tilde{d}$). Since the factors $f(L_e/d_c)$, $F_r(p,N)$, and $F_\parallel(p,N)$ are weak functions of the polymer molecular weight, the molecular weight dependence of $\tilde{B}$ is essentially determined by $\tilde{L}_e^{\,4}/N$.

6. Comparison with Experimental Data of η_0

The viscosity equations 14a and 14b must be tested with the experimental data of η_0 for well-characterized samples with narrow molecular weight distributions in wide ranges of the involved parameters, c, M, and q. There are rather few data for stiff-chain polymers that satisfy these conditions. Here we choose for this test the η_0 data of Enomoto et al.[2] for schizophyllan and of Takada et al.[1] for xanthan (the preceding paper). These polymers are rigid helical polysaccharides and have been characterized well from dilute solution studies; q = 120 nm, d = 2.2 nm, and the molecular weight per unit contour length M_L = 1940 nm^{-1} for xanthan in 0.1 M aqueous sodium chloride (NaCl),[32] while q = 200 nm, d = 2.6 nm, and M_L = 2140 nm^{-1} for schizophyllan in water.[33] Schizophyllan is stiffer than xanthan.

The reduced viscosity H_e can be calculated from η_0 and $[\eta]$, determined experimentally, if $\gamma\chi^2$ is known. Since there is no hydrodynamic calculation of γ and χ for the wormlike cylinder, we use those of the straight spherocylinder calculated by Yoshizaki and Yamakawa[29] (cf. Appendices A and B), although the neglect of the flexibility effect on γ and χ might introduce some error in H_e for samples with large N.

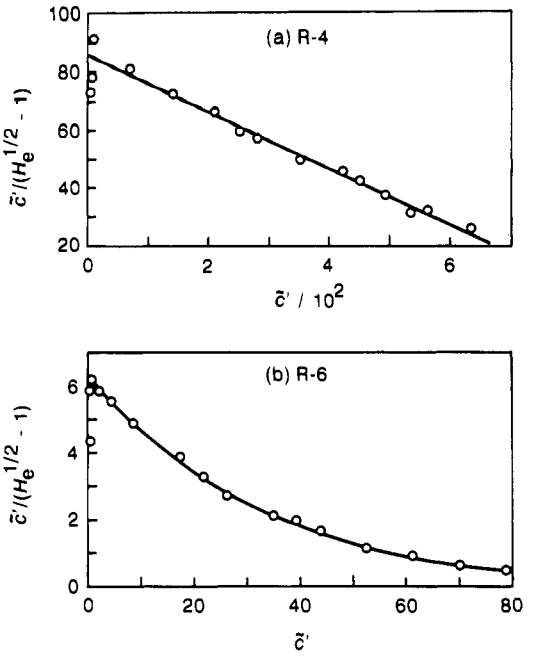

Figure 3. Test of eq 14a with data for aqueous solutions of the xanthan with 0.1 M NaCl at 25 °C; (a) sample R-4 with N = 1.27; (b) sample R-6 with N = 4.08.

Figure 3a shows the plots of $\tilde{c}'/(H_e^{1/2} - 1)$ vs $\tilde{c}'$ constructed from viscosity data for the xanthan sample with N = 1.27 in 0.1 M aqueous NaCl. The data points almost follow the indicated straight line, as predicted by eq 14a. However, in Figure 3b, the same plot for the xanthan sample with N = 4.08 in 0.1 M aqueous NaCl does not obey a straight line but a curve convex downward.[34] Examining the η_0 data for all the xanthan and schizophyllan samples studied, we find that the solution viscosity only for samples with $N \lesssim 2$ shows the concentration dependence given by eq 14a.[35] The failure of eq 14a for larger N may be attributed to the breakdown of the assumption that the hindrance of the longitudinal motion of a chain by surrounding chains is released only by the longitudinal diffusion of the hindering chains. When the chain has sufficient flexibility, internal conformation changes of the diffusing and/or hindering chains may also open a path for the longitudinal diffusion of the chain. This release mechanism has not been considered in the Green function formulation giving eq 8a and then eq 14a.

Figure 4 shows the plots of ln $[(H_e^{1/2} - 1)/\tilde{c}']$ vs $\tilde{c}'$ for three xanthan samples with N = 0.25, 4.08, and 11.6 in 0.1 M aqueous NaCl. For each sample, the data points follow closely the straight line indicated. This linearity was observed also for all the other xanthan samples presented in the previous paper and for aqueous schizophyllan with $0.15 \lesssim N \lesssim 5.02$, two of which are shown in Figure 5. These linear plots demonstrate that the viscosity equation (14b) obtained from the hole theory for $D_\parallel$ can describe well the concentration dependence of η_0 for two kinds of stiff polymer solutions over the wide ranges of the polymer concentration and N examined.

The linearity of the plot as found in Figures 4 and 5 allows us to estimate $\tilde{B}$ and $\tilde{V}_{ex}^*$ from the ordinate intercept and slope, respectively, according to eq 14b. Figure 6 shows the values of $\tilde{B}(F_r/F_\parallel)^{1/2}$ thus estimated vs N for the xanthan solutions (filled circles) and schizophyllan solutions (open circles), with the values of F_r and $F_\parallel$ being calculated by eqs A7 and A12, respectively. The data points for both

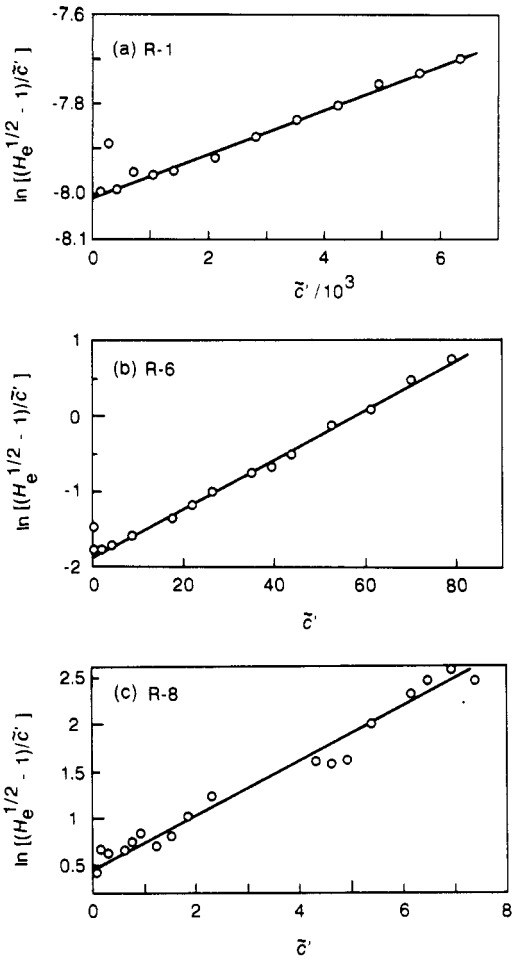

Figure 4. Test of eq 14b with data for aqueous solutions of xanthan with 0.1 M NaCl at 25 °C: (a) sample R-1 with $N = 0.25$; (b) sample R-6 with $N = 4.08$; (c) sample R-8 with $N = 11.6$.

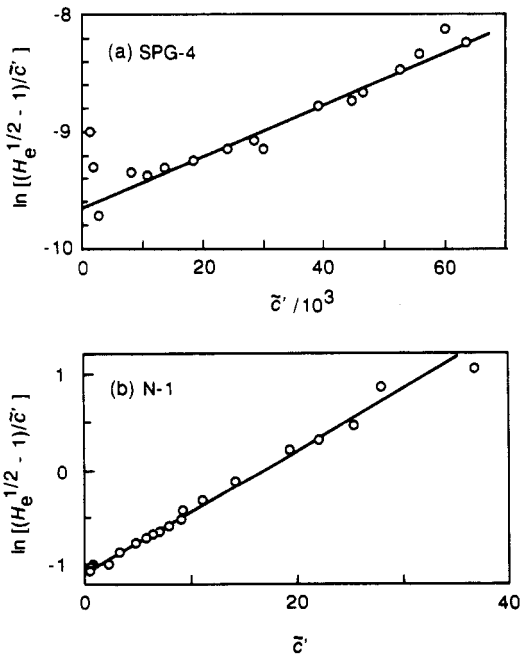

Figure 5. Same test as in Figure 4 but with data for aqueous solutions of schizophyllan at 30 °C: (a) sample SPG-4 with $N = 0.15$; (b) sample N-1 with $N = 5.02$.

polymer solutions appear to form a single composite curve. In the same figure are compared the theoretical values of $\tilde{B}(F_r/F_\parallel)^{1/2}$ calculated by eq 15; the solid and dot-dash curves are for d_c equal to 0 and d_e, respectively, along with

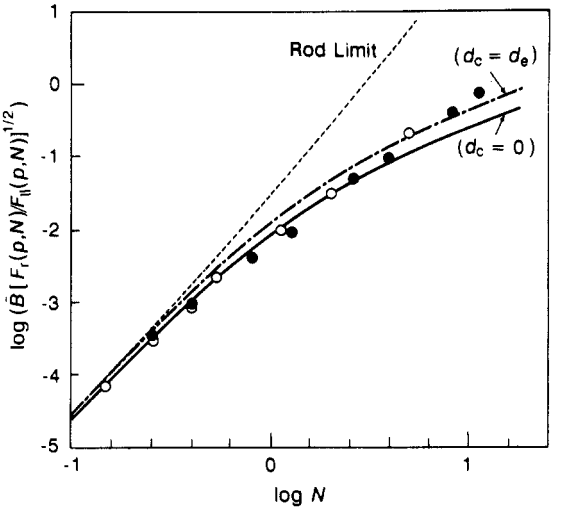

Figure 6. Double-logarithmic plot of $\tilde{B}[F_r(p,N)/F_\parallel(p,N)]^{1/2}$ vs N for aqueous solutions of xanthan (filled circles) and schizophyllan (unfilled circles). The solid and dot-dash curves represent the theoretical values calculated from eq 15 with $d_c = 0$ and d_e, respectively; the dashed curve shows the theoretical values for the rigid rod.

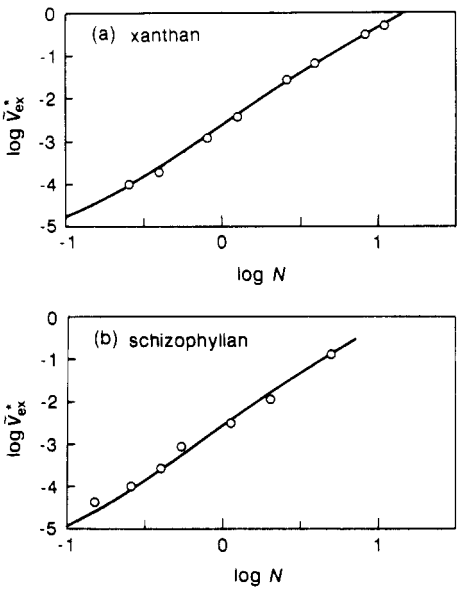

Figure 7. Double-logarithmic plot of $\tilde{V}_{ex}^*$ vs N for aqueous solutions of xanthan (a) and schizophyllan (b). The solid curve in each part represents the value calculated from eq 17 with $\lambda^* = 0.11$ (a) and 0.13 (b).

$\beta = 1350$, the value evaluated by Teraoka et al.,[24] whereas the dashed curve is for the "rod" limit, which is obtained from $\tilde{B}$ calculated by eq 15 with $L_e = N$, $d_c = 0$, N (in F_r and $F_\parallel$) = 0, and $\beta = 1350$. The data points for both polymers follow closely the solid curve for N below 4. At larger N, the data points for both polymers appear rather closer to the dot-dash curve. However, the theoretical values are not very sensitive to the choice of d_c; the ratio of $\tilde{B}(F_r/F_\parallel)^{1/2}$ between the two choices does not exceed 1.8 at $N = 10$, and d_c is not so important a parameter in η_0. On the other hand, the Rod limit curve begins to deviate definitely above the data points at N as small as 0.5. This manifests itself a remarkable effect of the chain flexibility on η_0. In Part 1,[10] we obtained a β of 4400, about 3 times larger than that of Teraoka et al.[24] This overestimation is mainly due to the neglect of this strong flexibility effect. (The neglect of the finite thickness effect of rods in Part 1 also contributes to this overestimation of β.)

Figure 7 displays the double-logarithmic plots of $\tilde{V}_{ex}^*$ (the mutual excluded volume between the critical hole and the solute molecule) vs N for aqueous solutions of the two polysaccharides. In each panel, the data points follow a weakly sigmoidal curve. Next we show that this experimentally found N dependence of $\tilde{V}_{ex}^*$ can be described well if we assume that the critical hole is similar to the diffusant or fuzzy cylinder; i.e., both have same shape but different sizes. Let $\tilde{L}^*$ and $\tilde{d}^*$ be the length and diameter of the critical hole, which are respectively equal to

$$\tilde{L}^* = \lambda^* \tilde{L}_e, \quad \tilde{d}^* = \lambda^* \tilde{d}_e \tag{16}$$

with λ^* being the similitude ratio of the critical hole and fuzzy cylinder. On the other hand, the solute molecule is a wormlike cylinder with the length N and the diameter $\tilde{d}$. Since the flexibility effect on the excluded volume is rather weak,[28] $\tilde{V}_{ex}^*$ may be calculated by utilizing Onsager's formula for the mutual excluded volume between cylinders with different sizes[23] as

$$\tilde{V}_{ex}^* = \frac{\pi}{4}\Big[N\tilde{L}^*(\tilde{d} + \tilde{d}^*) + (N\tilde{d}^2 + \tilde{L}^*\tilde{d}^{*2}) + \frac{1}{2}(N\tilde{d}^{*2} + \tilde{L}^*\tilde{d}^2) + \frac{\pi}{2}(N + \tilde{L}^*)\tilde{d}\tilde{d}^* + \frac{\pi}{4}(\tilde{d} + \tilde{d}^*)\tilde{d}\tilde{d}^* \Big] \tag{17}$$

The solid curves in Figure 7 are drawn from eq 17 with $\lambda^* = 0.11$ for xanthan (a) and $\lambda^* = 0.13$ for schizophyllan (b). For both polymers, the solid curves fit the data points well over the whole range of N examined. The similitude between the critical hole and the diffusant in semiflexible polymer solutions may be compared with the proportionality between the critical free volume and the real volume of small molecules and ions in the liquid state found by Cohen and Turnbull,[12] who studied the self-diffusion in liquids.

In conclusion, the viscosity equation (14b) along with eqs 15–17 can describe well the polymer concentration and molecular weight dependences of η_0 for stiff polymer solutions from dilute through concentrated isotropic at least with $N < 12$. As a further confirmation of the present conclusion, the viscosity data for the other stiff-chain polymer solutions should be compared with the viscosity equation. In addition, a similar critical test of eqs 6 and 8 may be made with experimental data for the rotational and translational self-diffusion coefficients of stiff polymers at finite concentration, although for the latter we also need an expression for the transverse diffusion coefficient of the stiff chain. These tests will be presented in future publications.

Acknowledgment. This work was financially supported by a Grant-in-Aid for Scientific Research (No. 01470108) from the Ministry of Education, Science, and Culture of Japan.

Appendix A. Transport Coefficients of Wormlike Chains in Dilute Solution

From the Oseen–Burgers procedure of hydrodynamics, the longitudinal diffusion coefficient $D_{\parallel 0}$, rotational diffusion coefficient D_{r0}, and intrinsic viscosity $[\eta]$ of very thin rods in dilute solution are given by[36-38]

$$D_{\parallel 0} = (k_B T/2\pi\eta_s L)(\ln p) \tag{A1}$$

$$D_{r0} = (3k_B T/\pi\eta_s L^3)(\ln p) \tag{A2}$$

$$[\eta] = (2N_A/15\eta_s M)(k_B T/D_{r0}) \tag{A3}$$

where L, p, and M are the length, axial ratio, and molecular weight of the rodlike polymer, respectively, and N_A is Avogadro's number. These relations have been used in Part 1[10] to formulate D_r and η_0 of rodlike polymers in isotropic solution without correction for the finite thickness effect of rods. In this appendix, we present approximate expressions of these transport coefficients of wormlike cylinders with finite thicknesses in dilute solution.

Yamakawa and Yoshizaki[39] evaluated the mean translational diffusion coefficient D_{t0} of the wormlike and helical wormlike cylinder in dilute solution by the Oseen–Burgers procedure. The result for the wormlike cylinder is represented in the form

$$D_{t0} = (k_B T/3\pi\eta_s L)\bar{s}_{a\text{-}KP}(N,\tilde{d};\sigma_1) \tag{A4}$$

where $\bar{s}_{a\text{-}KP}(N,\tilde{d};\sigma_1)$ is given by eq 25 of ref 39 with $c_\infty = 1$ and $\sigma_1 = 2.278$. (To be consistent with our notation in the text, L and d in ref 39 should be replaced by $N = L/2q$ and $\tilde{d} = d/2q$, where q and d are the persistence length and diameter of the wormlike cylinder, respectively.) Since D_{t0} is expressed by the longitudinal and transverse diffusion coefficients $D_{\parallel 0}$ and $D_{\perp 0}$ by

$$D_{t0} = (1/3)(D_{\parallel 0} + 2D_{\perp 0}) \tag{A5}$$

$D_{\parallel 0}$ is given by

$$D_{\parallel 0} = (k_B T/2\pi\eta_s L)F_{\parallel}(p,N)^{-1} \tag{A6}$$

with

$$F_{\parallel}(p,N)^{-1} = 2\bar{s}_{a\text{-}KP}/(1 + 2D_{\perp 0}/D_{\parallel 0}) \tag{A7}$$

($p = L/d = N/\tilde{d}$). Since the ratio $D_{\perp 0}/D_{\parallel 0}$ has not been formulated for the wormlike cylinder, we make an approximate estimate of the ratio by replacing the wormlike cylinder by an ellipsoid of revolution with the aspect ratio $p_e \equiv L_e/d_e$. For the ellipsoid, the ratio is given by[40]

$$D_{\perp 0}/D_{\parallel 0} = \frac{1}{2}\frac{(p_e^2 - 3/2)I_x + p_e^2}{(p_e^2 - 1/2)I_x - p_e^2} \tag{A8}$$

with

$$I_x = \frac{2p_e}{(p_e^2 - 1)^{1/2}}\cosh^{-1} p_e \tag{A9}$$

where $L_e = \langle R^2\rangle^{1/2}$ and d_e is estimated from eq 1. When $p_e \geq \sqrt{6}$, the factor $(1 + 2D_{\perp 0}/D_{\parallel 0})/3$ is in the range from 0.667 to 0.842, so that its value is not very important, and the replacement of the wormlike cylinder by the ellipsoid of revolution may not yield a serious error in eq A6 with eq A7.

Yoshizaki and Yamakawa[29] also calculated D_{r0} and $[\eta]$ of spheroid-cylinder molecules in dilute solution and obtained the relation

$$D_{r0} = \frac{2N_A k_B T}{15\eta_s M[\eta]}\gamma^{-1} \tag{A10}$$

where γ is a function of p and calculated from eq 138 along with eqs 121 and 128 of ref 29 (ϵ in the equations is taken to be unity). Further, Yamakawa and Yoshizaki[41] calculated $[\eta]$ of the wormlike and helical wormlike cylinders

by the same method as D_{t0}. The result $[\eta]_{KP}$ of the wormlike cylinder is a function of N and p, given by eqs 23 and 25 of ref 41 ($\epsilon = 1$). (It should be noticed that, in their theory, all lengths are measured in units of $2q$.) We estimate D_{r0} of the wormlike cylinder from their $[\eta]_{KP}$ using eq A10; i.e.

$$D_{r0} = (3k_BT/\pi\eta_s L^3)F_r(p,N)^{-1} \tag{A11}$$

with

$$F_r(p,N) = \frac{45M[\tilde{\eta}]_{KP}}{2\pi N_A N^3}\gamma \tag{A12}$$

where $[\tilde{\eta}]_{KP} = [\eta]_{KP}/(2q)^3$ and $N = L/2q$ and correspond, respectively, to $[\eta]_{KP}$ and L in ref 41. To a first approximation, γ for the straight spherocylinder[29] is used in the above estimation of D_{r0}, and the flexibility effect on γ is not considered, although it may cause some error in $F_r(p,N)$ at large N.

Appendix B. Finite Thickness Correction to the Relation between η_0 and D_r of Rodlike Polymer Solutions

Doi and Edwards[17] divided the stress tensor of rodlike polymer solutions into the viscous and elastic terms and obtained the relation between η_0 and D_r, which is valid to any concentration range of isotropic solution (see eqs 8.134, 9.54, 9.55, and 10.84 of ref 17)

$$\eta_0 = \eta_s + \frac{c'k_BT}{30D_{r0}} + \frac{c'k_BT}{10D_r} \tag{B1}$$

where the second and third terms correspond to the viscous and elastic stresses, respectively. (Equation 10.84 of ref 17, which contains only the elastic stress term, has the numerical factor of $^1/_6$ instead of $^1/_{10}$. However, if we do not adopt the decoupling approximation, this equation also coincides with eq B1.) In Part 1,[10] this equation has been used to obtain a viscosity equation of rodlike polymer solutions.

At infinite dilution, eq B1 is reduced to the relation between $[\eta]$ and D_{r0}, while the third term due to the elastic stress gives the frequency-dependent term $[\eta]_\omega$ of the dynamic intrinsic viscosity.[17,29] Since Doi and Edwards did not consider the end effect or finite thickness effect, eq B1 gives the Kirkwood–Auer relation[37] (eq A3), which is known to be valid only for infinitely thin (or long) rods. On the other hand, Yoshizaki and Yamakawa[29] evaluated $[\eta]$ and $[\eta]_\omega$ of spheroid cylinders considering the end effect of cylinders. The former is given by eq A10, while the latter is written as

$$[\eta]_\omega = \frac{N_Ak_BT}{10M\eta_sD_{r0}}\chi^2 \tag{B2}$$

where χ is another correction factor which depends on p and can be calculated from eq 133 of ref 29.

We have modified eq B1 so that it gives eq A10 for $[\eta]$ and eq B2 for the elastic term of $[\eta]$ or $[\eta]_\omega$ at infinite dilution. The modified equation is given by eq 10 in the text. Here we have assumed that γ and χ are independent of the polymer concentration.

References and Notes

(1) Takada, Y.; Sato, T.; Teramoto, A. *Macromolecules*, preceding paper in this issue.
(2) Enomoto, H.; Einaga, Y.; Teramoto, A. *Macromolecules* **1984**, *17*, 1573; **1985**, *18*, 2695.
(3) Maguire, J. F.; Mctague, J. P.; Rondelez, F. *Phys. Rev. Lett.* **1980**, *45*, 1891.
(4) Zero, K. M.; Pecora, R. *Macromolecules* **1982**, *15*, 87.
(5) Odijk, T. *Macromolecules* **1983**, *16*, 1340.
(6) Doi, M. *J. Polym. Sci., Polym. Symp.* **1985**, *73*, 93.
(7) Itou, T.; Teramoto, A. *Macromolecules* **1988**, *21*, 2225.
(8) Mori, Y.; Ookubo, N.; Hayakawa, R.; Wada, Y. *J. Polym. Sci., Polym. Phys. Ed.* **1982**, *20*, 2111.
(9) Odell, J. A.; Atkins, E. D. T.; Keller, A. *J. Polym. Sci., Polym. Lett. Ed.* **1983**, *21*, 289.
(10) Sato, T.; Teramoto, A. *Macromolecules* **1991**, *24*, 193.
(11) Edwards, S. F.; Evans, K. E. *J. Chem. Soc., Faraday Trans. 2* **1982**, *78*, 113.
(12) Cohen, M. H.; Turnbull, D. *J. Chem. Phys.* **1959**, *31*, 1164.
(13) Altenberger, A. R.; Dahler, J. S.; Tirrell, M. *Macromolecules* **1988**, *21*, 464.
(14) Freed, K. F.; Edwards, S. F. *J. Chem. Phys.* **1974**, *61*, 3626.
(15) de Gennes, P.-G. *Macromolecules* **1976**, *9*, 594.
(16) Muthukumar, M.; Edwards, S. F. *Macromolecules* **1983**, *16*, 1475.
(17) Doi, M.; Edwards, S. F. *The Theory of Polymer Dynamics*, Clarendon: Oxford, 1986.
(18) Kratky, O.; Porod, G. *Recl. Trav. Chim. Pays-Bas* **1949**, *68*, 1106.
(19) Hoshikawa, H.; Saitô, N.; Nagayama, K. *Polym. J.* **1975**, *7*, 79.
(20) Tagami, Y. *Macromolecules* **1969**, *2*, 8.
(21) Hearst, J. E. *J. Chem. Phys.* **1963**, *38*, 1062; **1964**, *40*, 1506.
(22) Teraoka, I.; Hayakawa, R. *J. Chem. Phys.* **1989**, *91*, 2643.
(23) Onsager, L. *Ann. N.Y. Acad. Sci.* **1949**, *51*, 627.
(24) Teraoka, I.; Ookubo, N.; Hayakawa, R. *Phys. Rev. Lett.* **1985**, *55*, 2712.
(25) Ogston, A. G. *Trans. Faraday Soc.* **1958**, *54*, 1754.
(26) Jansons, K. M.; Phillips, C. G. *J. Colloid Interface Sci.* **1990**, *137*, 75 and references therein.
(27) As pointed out by Jansons and Phillips,[26] eq 9 is obtained on the assumption that surrounding solute molecules in solution are distributed independently, i.e., not correlated with each other. The same assumption has been used in the mean-field Green function formulations of D_r and $D_\parallel$.
(28) Khokhlov, A. R.; Semenov, A. N. *Physica A* **1981**, *108*, 546; **1982**, *112*, 605. Odijk, T. *Macromolecules* **1986**, *19*, 2313.
(29) Yoshizaki, T.; Yamakawa, H. *J. Chem. Phys.* **1980**, *72*, 57.
(30) Nagasaka, K.; Yamakawa, H. *J. Chem. Phys.* **1985**, *83*, 6480.
(31) Roitman, D. B.; Zimm, B. H. *J. Chem. Phys.* **1984**, *81*, 6333.
(32) Sato, T.; Norisuye, T.; Fujita, H. *Macromolecules* **1984**, *17*, 2696.
(33) Yanaki, T.; Norisuye, T.; Fujita, H. *Macromolecules* **1980**, *13*, 1462.
(34) The nonlinearity of the plot shown in Figure 3b is not attributed to the neglect of the flexibility effects on γ and χ, because the quantity $H_e^{1/2} - 1$ can be approximated by $[4(\eta_c - 1)/3\gamma\chi^2]^{1/2}$ except for very dilute solutions, and the error in $\gamma\chi^2$ does not affect the concentration dependence given by eq 14a for nondilute solutions.
(35) When N is less than 2, $\tilde{B}$ and $\tilde{d}_c/\alpha$ are estimated from the intercept and slope of the linear plot of $\tilde{c}'/(H_e^{1/2} - 1)$ vs $\tilde{c}'$. For both polymers, the molecular weight or N dependence of $\tilde{B}$ obtained agrees with eq 15, while $\tilde{d}_c/\alpha$ is equal to about $\tilde{d}/11$ at $N \lesssim 0.4$ and increases with N at $0.4 \lesssim N$ (<2).
(36) Burgers, J. M. In *Second Report on Viscosity and Plasticity of the Amsterdam Academy of Sciences*; Nordemann: New York, 1938; Chapter 3.
(37) Kirkwood, J. G.; Auer, P. L. *J. Chem. Phys.* **1951**, *19*, 281.
(38) Yamakawa, H. *Macromolecules* **1975**, *8*, 339.
(39) Yamakawa, H.; Yoshizaki, T. *Macromolecules* **1979**, *12*, 32.
(40) Lamb, H. *Hydrodynamics*, 6th ed.; Cambridge University Press: Cambridge, U.K., 1932; p 604.
(41) Yamakawa, H.; Yoshizaki, T. *Macromolecules* **1980**, *13*, 633.

Registry No. Schizophyllan, 9050-67-3; xanthan, 11138-66-2.